Blends of Amphiphilic PDMS and Trisilanolisobutyl-POSS at the Air/Water Interface

John R. Hottle,[†] Hyong-Jun Kim,[†] Jianjun Deng,[†] Catherine E. Farmer-Creely,[†,§] Brent D. Viers,[‡] and Alan R. Esker*[,†]

Department of Chemistry, Virginia Polytechnic Institute and State University, Blacksburg, Virginia 24061, and ERC/PRSM, Air Force Research Laboratories, Edwards Air Force Base, California 93524

Received March 11, 2004; Revised Manuscript Received April 21, 2004

ABSTRACT: Blends of amphiphilic poly(dimethylsiloxane) (PDMS) and a model polyhedral oligomeric silsesquioxane (POSS) nanofiller, trisilanolisobutyl-POSS, form homogeneous monolayers at the air/water interface. At high POSS content (>80 wt %), a thermodynamic analysis of surface pressure−area per monomer (Π−*A*) isotherm data suggests possible phase separation prior to collapse of the PDMS component. PDMS bilayer formation that normally occurs around $\Pi \approx 8$ mN m^{-1} shifts to higher surface pressures with increasing trisilanolisobutyl-POSS content, indicating compatibility between the two materials in the monolayer state that is analogous to a positive deviation binary liquid mixture. Further compression leads to the collapse of the POSS component into multilayer domains around $\Pi \approx 17.5$ mN m^{-1}. Brewster angle microscopy shows the amount of PDMS in the blend alters the aggregation state of the nonequilibrium solidlike trisilanolisobutyl-POSS domains. These results provide insight into POSS aggregation mechanisms that may be present in thicker films and bulk systems.

Introduction

Over the past decade, polyhedral oligomeric silsesquioxane (POSS) molecules have attracted considerable attention. With rigid inorganic cores and flexible organic coronae of nanometer dimensions,[1,2] POSS molecules have been used for hybrid organic−inorganic nanocomposites,[3,4] space-survivable coatings,[5,6] and synthetic templates for nanostructured materials.[7−12] The polyhedral silicon−oxygen nanostructured skeleton, from which the name is derived, consists of intermittent siloxanes of the general formula $(SiO_{3/2})_n$,[13−17] which was first reported in 1946.[18] By incorporating POSS into polymeric species, improved physical properties such as low-*k* dielectric constants,[19−21] high glass transition temperatures (T_g),[22,23] high thermal stability,[24−26] high oxidation resistance,[5,6] photoresists,[27,28] and unique crystalline materials[29,30] can be obtained.

POSS molecules, representing hybrid organic−inorganic materials with a core−shell structure, can be thought of as the smallest possible particles of silica.[1,2] While the interfacial properties are important for future applications of POSS, relatively little is actually known about the surface properties of POSS systems.[31−33] Recently, Deng et al. showed that the partial cage structure of trisilanolisobutyl-POSS, $T_7R_7(OH)_3$ where R = isobutyl, can form stable Langmuir monolayers.[34,35] In view of the physical structure of POSS, with small length/diameter ratios and barrel-like shapes, one can imagine trisilanol-POSS molecules will have simpler monolayer phase behavior than fatty acids. Hence, POSS molecules may afford the opportunity to study interactions between polymers and nanofillers in a "two-dimensional" Langmuir monolayer system.

This report focuses on the compatibility of two amphiphiles, trisilanolisobutyl-POSS[34,35] and poly(dimethylsiloxane) (PDMS),[36] as blended films at the air/water interface (A/W) by monitoring their interactions with the Wilhelmy plate technique and Brewster angle microscopy (BAM). PDMS was first reported to have surface-active properties in 1947.[36] Since then, studies have been performed to show the formation of monolayer and multilayer films at A/W.[37−39] In this study the entire composition range, 0−100 wt % PDMS, is examined as blends with trisilanolisobutyl-POSS. This study provides a detailed examination of the monolayer and collapse behavior of mixtures of trisilanolisobutyl-POSS with PDMS at A/W.

Experimental Section

Materials. Trisilanolisobutyl-POSS (HybridPlastics, Inc.) and PDMS ($M_n = 7.5$ kg/mol, $M_w/M_n = 1.09$, Polymer Source, Inc.) were used without further purification. Spreading solutions were made by dissolving the pure components or blends in chloroform (≈0.5 mg mL^{-1}, HPLC grade). The samples were allowed to dissolve for more than 24 h.

Isotherm Studies. The blend was spread onto the surface of a standard Langmuir trough (500 cm^2, Nima Technology, 601BAM) filled with ultrapure 18.2 MΩ water (Millipore, Milli-Q Gradient A-10) maintained at 22.5 °C in a Plexiglas box with a relative humidity of 70−75%. To investigate the thermodynamic properties of the trisilanolisobutyl-POSS/PDMS mixtures, four methods were used to vary the surface area or surface concentration: (1) "compression" of the barriers at a constant rate, (2) successive "addition" of spreading solution, (3) "hysteresis" loops, and (4) "relaxation" (the portions in quotation marks indicate the short form used throughout the paper). For compression at a constant rate, each sample was compressed at 20 cm^2 min^{-1}. For hysteresis, each sample was compressed at a speed of 20 cm^2 min^{-1} to a designated average area per monomer value, $\langle A \rangle$, and were immediately expanded at the same speed to a final trough area of 480 cm^2. This method was used to test the reversibility of the different structural stages of the film. For successive addition, the surface area was held constant and the surface concentration was varied by making successive additions of

[†] Virginia Polytechnic Institute and State University.
[‡] ERC/PRSM, Air Force Research Laboratories.
[§] Present address: Department of Chemistry, The Catholic University of America, Washington, DC 20064.
* To whom correspondence should be addressed.

10.1021/ma049511m CCC: $27.50
Published on Web 06/03/2004

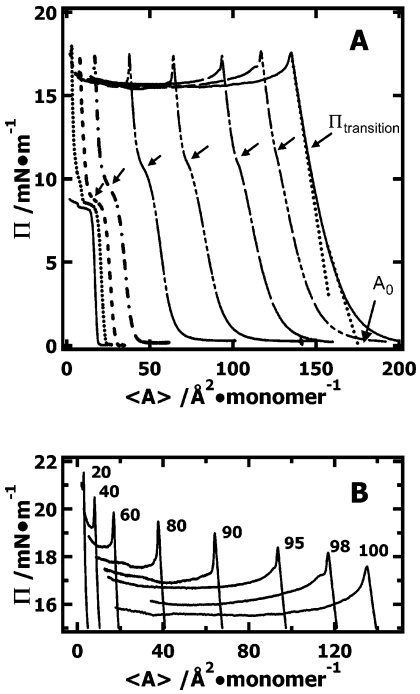

Figure 1. (A**)** Π−⟨*A*⟩ compression isotherms for trisilanolisobutyl-POSS blends with PDMS. Temperature was held constant at 22.5 °C, and a compression rate of 20 cm^2 min^{-1} was used. The amount of POSS (wt %) is 0, 20, 40, 60, 80, 90, 95, and 100 from left to right, respectively. The arrows indicate the composition-dependent transition surface pressure, $\Pi_{transition}$, for PDMS multilayer formation. The linear dotted lines are used to show the extrapolation to the cross-sectional area, A_0 = 175 Å^2 monomer^{-1}, at low Π and the start of the "nonequilibrium" regime at higher Π for the pure trisilanolisobutyl-POSS isotherm. **(B)** The isotherms in (A) have been replotted whereby each isotherm is offset from the previous isotherm by an additional +0.5 mN m^{-1} (+3.5 mN m^{-1} total offset for the 20 wt % POSS film from the unaltered 100 wt % POSS film) with decreasing POSS content to highlight the plateau region.

spreading solution. After each addition, Π was allowed to relax to a constant minimum value (ΔΠ < 0.1 mN m^{-1} over a 10 min period) after evaporation of the spreading solvent. For low surface pressures, the total relaxation time including solvent evaporation was on the order of 20−30 min, while times on the order of an hour were necessary in the collapsed regime. For relaxation experiments, each sample was compressed at a speed of 20 cm^2 min^{-1} to a final compressed area per POSS molecule, $A_{POSS} \approx 60$ Å^2 monomer^{-1}. The barriers were held at that position, and the sample was allowed to relax. The surface pressure was recorded as a function of time until a constant value was observed. For all four methods, a minimum of 15 min was allocated after spreading to ensure the chloroform evaporated before all the isotherm measurements were started. Surface pressure, Π, was recorded by the Wilhelmy plate technique during all isotherm measurements. A completely wetted filter paper plate was used as the Wilhelmy plate.

Brewster Angle Microscopy (BAM). BAM studies (MiniBAM, NanoFilm Technologie GmbH, linear resolution better than or equal to 20 μm) were carried out simultaneously during the isotherm measurements, and the BAM images were taken by a CCD camera. The BAM images presented in this paper are 4.8 × 6.4 mm^2 unless specifically noted. The entire configuration (Langmuir trough, BAM, and Plexiglas box) rests on a floating optical table to minimize vibrations.

Results and Discussion

Compression Isotherm Studies of the Pure Components. Figure 1 shows a plot of surface pressure, Π, as a function of average area per monomer, ⟨*A*⟩, for different mixtures of PDMS and POSS. At dilute surface concentrations, ⟨*A*⟩ > 20 Å^2 monomer^{-1}, PDMS is known to form a liquid/gas (L/G) biphasic film.[39] In this regime, all of the Si and O atoms are able to adsorb to the subphase with the hydrophobic methyl substituents oriented into the air, reflecting the amphiphilic nature of PDMS. A liquidlike monolayer forms (14 < ⟨*A*⟩ < 18 Å^2 monomer^{-1}) forms upon film compression to ⟨*A*⟩ values less than the cross-sectional (limiting) area of a PDMS repeat unit (≈18 Å^2 monomer^{-1}). As Π increases in the monolayer regime, repeating units begin to pull out of the interface and collapse begins (first plateau, 9 < ⟨*A*⟩ < 14 Å^2 monomer^{-1}). At ⟨*A*⟩ ≈ 8 Å^2 monomer^{-1}, there is a smaller rise in Π followed by a second plateau (⟨*A*⟩ < 6 Å^2 monomer^{-1}). These transitions were originally described[36] in terms of helix formation; however, more recent studies suggest these are actually multilayer transitions where a "dry" PDMS layer spreads on top of a hydrated PDMS layer.[37] As it is not possible for the techniques used in this study to distinguish between the two cases, subsequent discussion will favor the multilayer model.

POSS also exhibits an interesting isotherm.[34,35] At low surface concentrations (⟨*A*⟩ > 220 Å^2 molecule^{-1}, not shown in Figure 1) Π ≈ 0 mN m^{-1}, and the film likely exists in a biphasic L/G coexistent regime;[35] with increasing compression (180 < ⟨*A*⟩ < 220 Å^2 molecule^{-1}) the POSS forms a liquidlike monolayer which shows no hysteresis during compression−expansion cycles.[35] Further compression in this regime leads to the formation of a less-compressible liquidlike monolayer (150 < ⟨*A*⟩ < 180 Å^2 molecule^{-1}), where extrapolation back to Π = 0 mN m^{-1} yields a limiting area of A_0 = 175 Å^2 molecule^{-1}, which is in excellent agreement with the known size of a different trisilanol-POSS derivative, trisilanolcyclohexyl-POSS, and molecular modeling of trisilanolisobutyl-POSS.[40] In this regime, the film only exhibits slight hysteresis during compression−expansion cycles. As the film is compressed further, there is another change in slope (135 < ⟨*A*⟩ < 150 Å^2 molecule^{-1}). In this regime, the film exists in a truly nonequilibrium state leading to the "cusp" in the isotherm at Π ≈ 17.5 mN m^{-1} (⟨*A*⟩ ≈ 135 Å^2 molecule^{-1}), signifying collapse of the film into multilayer domains. Addition and stepwise compression experiments both show that surface pressure values relax to Π ≈ 12.5 mN m^{-1}. Moreover, for Π > 17.5 mN m^{-1} the rapid formation of a more condensed phase causes a slight drop in Π until the barriers "catch up" because the multilayer phase that forms has a smaller area per molecule than in the monolayer state.

Compression Isotherm Studies of the Blends. Each isotherm, excluding the pure components (left-most curve = PDMS, right-most curve = POSS) represents a mixture with increasing weight percent POSS as you go from left to right in Figure 1. Qualitatively, the mixtures show behavior between the extremes of PDMS and POSS. For 0 < Π < 8 mN m^{-1}, a liquidlike monolayer is formed for all compositions. In the region 8 < Π < 13 mN m^{-1}, there is a composition-dependent collapse transition, $\Pi_{transition}$. This transition corresponds to PDMS multilayer formation. Above Π ≈ 13 mN m^{-1}, all blend isotherms exhibit POSS-like behavior and show an essentially composition independent cusp around Π ≈ 17.5 mN m^{-1}. The latter transition corresponds to the formation of POSS-rich multilayer do-

mains. After the cusp, the mixed isotherms show a long "plateau" as more POSS converts into multilayer domains. These features and their significance are discussed in more detail below.

The Monolayer Regime. Thermodynamic analysis of the isotherms can help to understand the mixing behavior at a molecular level. For $\Pi < 8$ mN m^{-1}, the appropriate expression for ideal mixing is given as

$$\langle A_{\mathrm{mix,ideal}}(\Pi)\rangle = X_{\mathrm{POSS}}A_{\mathrm{POSS}}(\Pi) + X_{\mathrm{PDMS}}A_{\mathrm{PDMS}}(\Pi) \quad (1)$$

where $A_{\mathrm{POSS}}(\Pi)$ and $A_{\mathrm{PDMS}}(\Pi)$ are the values of A at a given Π value for the pure component monolayers and X_{PDMS} and X_{POSS} are the mole fractions. Hence in 2-D, the analogous property to the volume change upon mixing in 3-D can be defined as

$$\Delta A_{\mathrm{mix}}(\Pi) = \langle A(\Pi)\rangle - \langle A_{\mathrm{mix,ideal}}(\Pi)\rangle \quad (2)$$

Figure 2A shows a plot of $\langle A(\Pi)\rangle$ vs the mole fraction of POSS in the blend films. Figure 2A shows representative data for two different Π values (2 and 7 mN m^{-1}) while comparable data for 5 mN m^{-1} were omitted for clarity. Surface pressure values below $\Pi = 8$ mN m^{-1} were chosen to avoid pressure-induced collapse of the PDMS component. Qualitatively, the data show positive deviation from ideal mixing ($\langle A_{\mathrm{mix,ideal}}(\Pi)\rangle$, the dotted lines on the figure). As positive deviation from ideal mixing indicates unfavorable enthalpic interactions, it is also useful to consider the molar Gibbs excess free energy of mixing, $\Delta G_{\mathrm{excess}}$, which can also be calculated from the $\Pi-A$ isotherms of the pure and mixed films:[41,42]

$$\Delta G_{\mathrm{excess}} = \int_0^{\Pi} \Delta A_{\mathrm{mix}}(\Pi)\, \mathrm{d}\Pi \quad (3)$$

The $\Delta G_{\mathrm{excess}}$ values for binary mixtures as a function of POSS mole fraction and surface pressure are shown in Figure 2B for $\Pi = 2$, 5, and 7 mN m^{-1}. For all the compositions studied, these curves were concave downward, giving positive $\Delta G_{\mathrm{excess}}$ values, in agreement with unfavorable interactions in binary monolayers.[42] These values become more positive with increasing surface pressure, indicating that the repulsion between the two components are stronger at larger Π. However, the near-zero values of $\Delta G_{\mathrm{excess}}$ observed for mixtures containing less than 80 wt % (≈27 mol %) POSS are consistent with uniphasic mixtures.[42] In contrast, mixtures containing larger amounts of POSS (>80 wt %, >27 mol %) have large $\Delta G_{\mathrm{excess}}$ values that may be consistent with phase separation. By assuming that the ideal entropy of mixing can be described by Flory−Huggins-type behavior, the Gibbs free energy of mixing, ΔG_{mix}, can be estimated as

$$\Delta G_{\mathrm{mix}}(\Pi) = \Delta G_{\mathrm{excess}}(\Pi) + \Delta G_{\mathrm{ideal}}(\Pi)$$

$$= \Delta G_{\mathrm{excess}}(\Pi) + \left(\phi_{\mathrm{POSS}} \ln \phi_{\mathrm{POSS}} + \frac{\phi_{\mathrm{PDMS}}}{n} \ln \phi_{\mathrm{PDMS}}\right) \quad (4)$$

where ϕ_i is the volume fraction of component i and n is the number of segments in a polymer chain based on the size of a solvent molecule (here $n = 101/8$).[43] These data are shown in Figure 2C for $\Pi = 2$ and 7 mN m^{-1} (5 mN m^{-1} data have been omitted for clarity), indicating that POSS/PDMS phase separation may occur just prior to the collapse transition of the film in POSS/PDMS mixtures containing more than 80 wt % POSS. However, no direct microscopic evidence was seen for this by BAM during compression, suggesting POSS and PDMS monolayers may have comparable thickness and refractive indices in this regime.

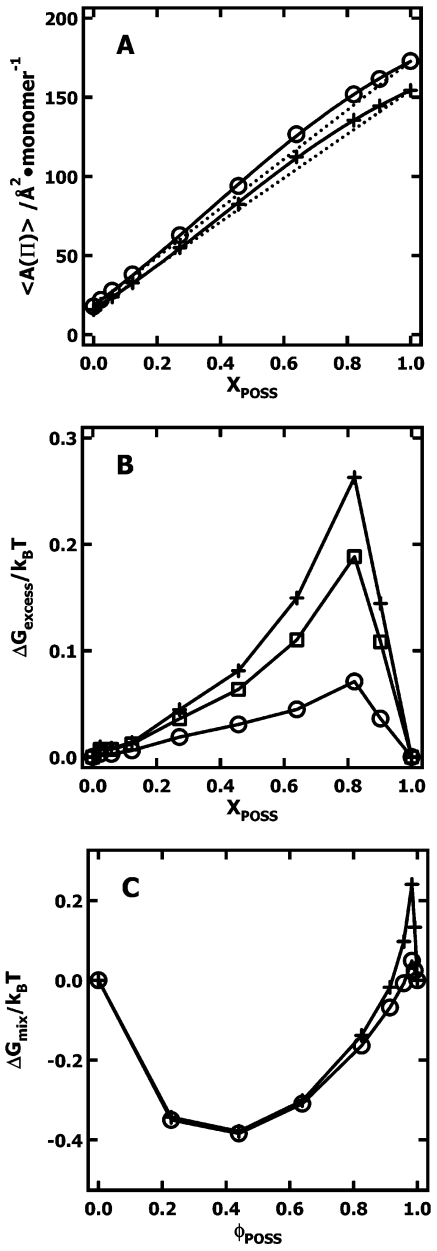

Figure 2. (A) Mean surface areas per repeating unit, (B) excess Gibbs free energies of mixing, and (C) estimated Gibbs free energies of mixing calculated from the isotherms at Π = 2 (○), 5 (□), and 7 mN m^{-1} (+) plotted as a function of the POSS mole fraction, X_{POSS}, or volume fraction, ϕ_{POSS}, on a monomer basis. Solid lines are guides for the eyes, and the dotted lines correspond to the values for ideal mixing. The Π = 5 mN m^{-1} data were omitted from (A) and (C) for clarity.

PDMS Collapse. The fact that the films show characteristics of both PDMS and POSS behavior requires a different treatment of the data for $\Pi > 8$ mN m^{-1}. PDMS undergoes a transition from a monolayer to a multilayer film around $\Pi \approx 8$ mN m^{-1}.[38] Whether this transition occurs through elaborate conformational changes as suggested by Fox et al.[36] or a simple spreading of "dry" PDMS on the top of the hydrated PDMS layer[37,38] is beyond the scope of this paper as both mechanisms would lead to a film that is roughly two

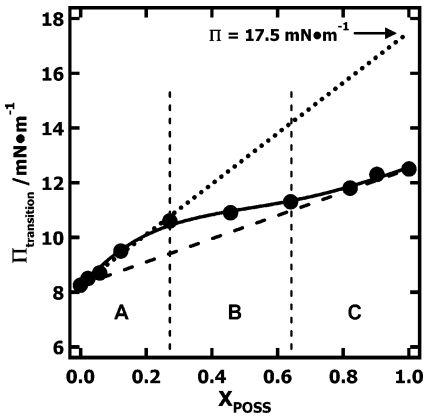

Figure 3. $\Pi_{transition}$ for PDMS multilayer formation as a function of the mole fraction of POSS on a per monomer basis. Filled circles (●) represent experimental data from Figure 1, the solid line is provided to highlight the trend, the bold dotted line represents ideal dilute solution behavior (Henry's law), and the dashed line connecting the "equilibrium" transition pressure of the pure components provides ideal solution behavior (Raoult's law). The vertical dashed lines are used to highlight the three distinct regimes (A, B, and C).

monomer units thick. In this study, the PDMS monolayer → multilayer transition manifests itself as a shoulder (shown as arrows in Figure 1) in the mixtures. This transition occurs at higher surface pressures in mixtures with increasing trisilanolisobutyl-POSS content. When the pressure is less than $\Pi_{transition}$, the films are monolayers and show average characteristics of PDMS and POSS. There is a positive deviation from ideal behavior over the entire composition range (Figure 2), ultimately similar to the partial pressure change of two dissimilar liquids.[44] The blend films at the water surface below $\Pi_{transition}$ are thought to be stable monolayers with both components staying at A/W, until the PDMS component is squeezed out of the interface due to a weaker water affinity than the POSS molecules—which is confirmed from the BAM studies and will be discussed later.

Above the shoulder in Figure 1, $\Pi_{transition}$ indicated by arrows, a different analysis is utilized. Figure 3 shows $\Pi_{transition}$ as a function of the mole fraction of POSS, X_{POSS}, calculated on a per monomer basis. The plot in Figure 3 can be thought of as a surface analogue to a vapor pressure diagram for an ideal-dilute binary mixture of volatile liquids, where the equilibrium collapse pressures of PDMS and POSS represent the vapor pressures of the pure components and the bold dashed line corresponds to the prediction of Raoult's law.[45] As seen in Figure 3, there are three distinct regimes. In region A, ideal-dilute solution behavior is observed with positive deviation from Raoult's law. The dotted line in Figure 3 provides the surface analogue of a Henry's law regime. By extrapolating the initial slope to pure POSS, one observes a value of $\Pi \approx 17.5$ mN m^{-1} or the dynamic collapse value of trisilanolisobutyl-POSS.[34,35] Hence, one observes a nonideal enhancement of the pressure-dependent stability of PDMS monolayers at low POSS loadings. In region B of Figure 3, deviations from Henry's law behavior are observed. By region C in Figure 3, Raoult's law behavior is observed with an extrapolation to $\Pi \approx 12.5$ mN m^{-1} for pure POSS. This value agrees amazingly well with the "thermodynamically" stable collapse value for trisilanolisobutyl-POSS.[35] Both the transition region, B, and the Raoult's law regime, C, are consistent with unfavorable interactions that may lead to phase separation. Therefore, a suitable interpretation may be that the presence of low-viscosity PDMS plasticizes the trisilanolisobutyl-POSS, thereby enhancing the rate at which it collapses, leading to a noticeable kink in the isotherm. Hence, region C should be characterized as the preferential collapse of the PDMS component with some collapsing POSS as well. In any event, these transitions occur in the absence of detectable reflectivity changes as the BAM images are homogeneous over the time scale of the compression.

The Nonequilibrium "Monolayer" Regime. Previous work with trisilanolisobutyl-POSS shows this POSS derivative forms a nonequilibrium monolayer between 12.5 and 17.5 mN m^{-1} upon compression.[35] In this regime, addition, stepwise compression, and compression isotherms yield different results as viscous trisilanolisobutyl-POSS monolayers collapse at a rate which is slower than the compression rate. As a result, continuous compression leads to a rise in Π until ultimate failure occurs with nonequilibrium collapse of the film at $\Pi \approx 17.5$ mN m^{-1}. As seen in Figure 1, this regime shifts to smaller $\langle A \rangle$ as the amount of PDMS increases. Nonetheless, neither increasing PDMS content nor the collapse of the PDMS component has a significant impact on the collapse pressure of the POSS component. Hence, the value of $\Pi \approx 17.5$ mN m^{-1} for nonequilibrium POSS collapse is a good measure for the dynamic affinity of trisilanolisobutyl-POSS at the surface for all PDMS compositions.

Collapse of the POSS Component. Unlike the collapse behavior at the shoulder, which corresponds to the monolayer → multilayer transition of PDMS, the surface pressure of the cusp, corresponding to the nonequilibrium formation of more condensed POSS domains, is unaffected by the amount of PDMS. This transition can be visualized with the aid of BAM as seen in Figure 4, where the solidlike domains appear brighter than the rest of the film. The micrographs in Figure 4 were chosen to ensure a constant POSS surface concentration of $A_{POSS} \approx 50$ Å^2 molecule^{-1}. This concentration is calculated by assuming the film is only composed of POSS. Pure trisilanolisobutyl-POSS only forms small nonequilibrium solidlike structures when compressed past the collapse pressure. Trisilanolisobutyl-POSS forms more solidlike multilayer domains for small amounts of added PDMS. It is possible that the greater area fraction of solid domains reflects a lower viscosity within the blend. Alternatively, PDMS could serve as a nucleation site for the heterogeneous formation of solidlike domains. These domains tend to aggregate into larger structures (Figure 4B). Ultimately, with increasing amounts of PDMS, the formation of solidlike POSS domains apparently becomes more difficult at a specific temperature and Π value as their surface fraction decreases (Figure 4D,E) as one might expect for the addition of a liquid solute. As noted above, there is definitely a larger surface fraction of multilayer domains present in the 90 wt % trisilanolisobutyl-POSS sample. The fact that multilayer domain formation and aggregation occur on a time scale that is initially faster than the rate of compression causes the pressure to drop slightly in the Π−*A* isotherms at the cusp prior to the formation of a long plateau that is observed upon compression past the cusp.

Hysteresis Studies. Once enough PDMS is incorporated into the blend films, the amount of solid present after the cusp decreases, and the compression becomes

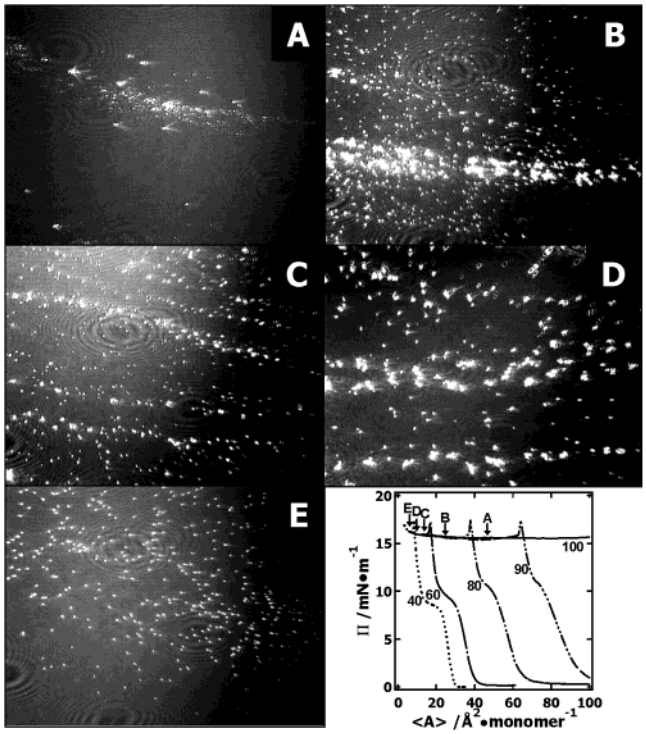

Figure 4. BAM images upon compression for different POSS/PDMS blends (wt % POSS, $\langle A \rangle$/Å^2 monomer^{-1}): A (100, 47.4), B (90, 25.4), C (80, 14.8), D (60, 9.5), and E (40, 6.4). The $\langle A \rangle$ values all correspond to a POSS concentration of $A_{POSS} \approx 50$ Å^2 molecule^{-1}. Solidlike domains appear bright in the images, which are 4.8 × 6.4 mm^2 in size. The letters on the $\Pi-\langle A \rangle$ isotherm show the positions where the BAM images were obtained.

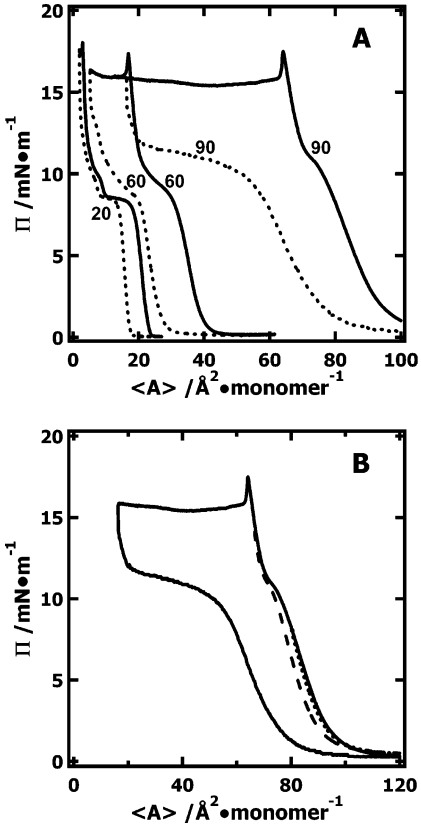

Figure 5. $\Pi-\langle A \rangle$ compression−expansion isotherms for single cycles of POSS/PDMS blends. All films were compressed and expanded at 20 cm^2 min^{-1} and a constant temperature of 22.5 °C. (A) Hysteresis curves for 20, 60, and 90 wt % POSS blends are shown from left to right. Solid curves represent the compression process, and the dashed curves represent the expansion process. (B) Hysteresis curves for a single composition, a 90 wt % POSS blend, compressed to $\Pi_{max} = 8$, 12, and 16 mN m^{-1}, corresponding to dotted, dashed, and solid expansion curves, respectively.

more reversible, as seen in Figure 5A. The sudden drop in Π upon expansion does not seem to depend on the amount of PDMS present in the blend. Three hysteresis cycles of POSS/PDMS blend films at A/W for fresh monolayers can be seen in Figure 5B for the 90 wt % POSS blend film. Three general conclusions can be drawn from Figure 5B for films at A/W: (1) a very stable reversible monolayer film forms below $\Pi \sim 7$ mN m^{-1}, i.e., before the PDMS component begins multilayer collapse; (2) irreversible PDMS bilayer formation occurs between 7 mN m^{-1} < Π < 17 mN m^{-1} as the respreading of PDMS from the bilayer state is slower than the rate of area expansion; and (3) unstable POSS multilayer domain formation occurs after the cusp, resulting in a two-step dynamic relaxation process corresponding to the respreading of POSS multilayer aggregates and subsequent respreading of PDMS. However, this respreading is incomplete. If multiple hysteresis loops are performed for the same monolayer, the results are strongly dependent on the maximum surface pressure value, Π_{max}, to which the monolayer is compressed. For Π_{max} < 7 mN m^{-1}, repeated loops are essentially identical. For 7 mN m^{-1} < Π_{max} < 17 mN m^{-1} there is a small shift in the curves to smaller $\langle A \rangle$ values (<5%) for the second and later cycles. However, for multiple cycling of films compressed deep into the collapsed regime of the POSS component, like the solid curve in Figure 5B, there is a continual shift to smaller $\langle A \rangle$ values for subsequent cycles from the preceding cycle (>10% per cycle dependent upon how far the film is compressed into the collapsed regime). This condition suggests that while solidlike POSS domains are no longer visible following the expansion of the film back to the initial $\langle A \rangle$ value, multilayer domains that are smaller than the resolution of the BAM must exist as subsequent recompression of the film requires smaller $\langle A \rangle$ values before the surface pressure rises. Moreover, the continual shift in $\langle A \rangle$ with increasing cycle number means that more of the film is converted into a "permanent" multilayer state with each cycle.

When there is a high concentration of trisilanolisobutyl-POSS present and a small amount of PDMS (<15 wt %), the area fraction of solid domains increases (Figure 4B). This feature may occur because the PDMS, when present in small amounts, functions as a nucleation site for the aggregation of trisilanolisobutyl-POSS and is possibly aided by phase separation as noted in the thermodynamic analysis of the monolayer regime. By utilizing BAM, the surface fraction and density of solidlike domains during expansion can be directly observed as seen in Figure 6. As more domains form for POSS films with small amounts of PDMS, a "spaghetti-like" network appears. The domains first appear as ring structures as seen in Figure 6B. As the trough area expands, these rings break apart into branched "spaghetti-like" strands as seen in Figure 6A and to a lesser extent in Figure 6C,D. The nucleation sites that allowed more solidlike domains to form also allow more network-like morphologies to form upon expansion of the barriers (Figure 6B). There is, however, a threshold on the amount of solid that will be formed with added

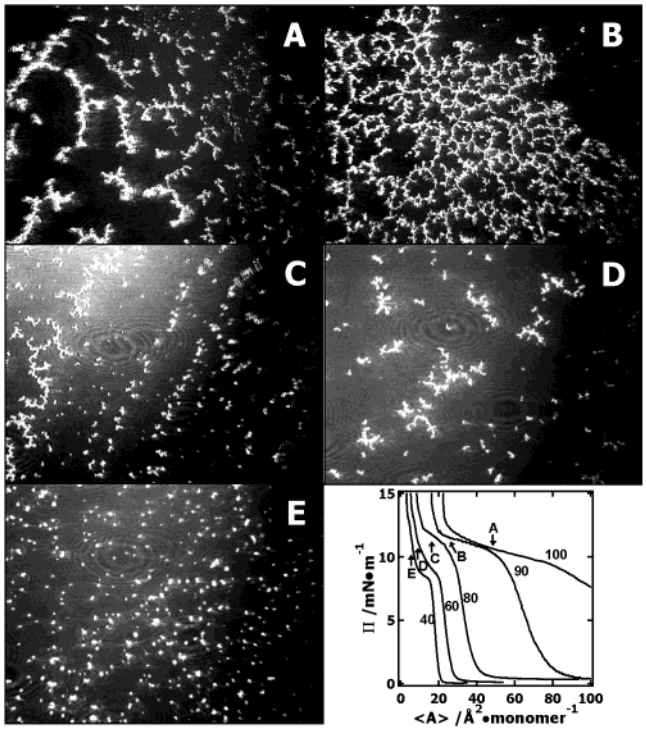

Figure 6. BAM images upon expansion for different POSS/PDMS blends (wt % POSS, $\langle A \rangle$/Å^2 monomer^{-1}): A (100, 49.5), B (90, 26.0), C (80, 14.0), D (60, 10.0), and E (40, 5.0). The $\langle A \rangle$ values all correspond to a POSS concentration of $A_{POSS} \approx 50$ Å^2 molecule^{-1}. Solidlike domains appear bright in the images, which are 4.8 × 6.4 mm^2 in size. The letters on the $\Pi-\langle A \rangle$ isotherm show the positions where the BAM images were obtained during the expansion process.

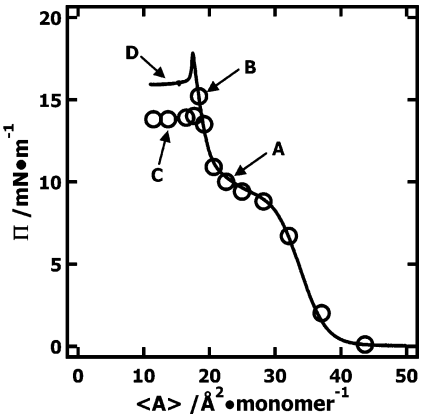

Figure 7. A $\Pi-\langle A \rangle$ isotherm comparison between addition and compression for a 60 wt % trisilanolisobutyl-POSS blend with PDMS. The compression isotherm (solid line) was obtained at 20 cm^2 min^{-1} at a temperature of 22.5 °C. The circles (○) represent "equilibrium" addition data. The letters correspond to the surface concentrations where BAM images shown in Figure 8 were obtained.

PDMS. As can be seen in Figure 4C−E, as more PDMS is introduced into the system, fewer domain structures form; hence, there are also fewer structures upon expansion (Figure 6C−E). Moreover, when network-like structures fail to form, the predominant morphology is one where most domains exist as small round structures (Figure 6E).

Addition Experiments. Figure 7 contains a representative comparison between compression data and data obtained by making successive additions of spreading solution for the 60 wt % trisilanolisobutyl-POSS blend with PDMS. After spreading, the surface pressure

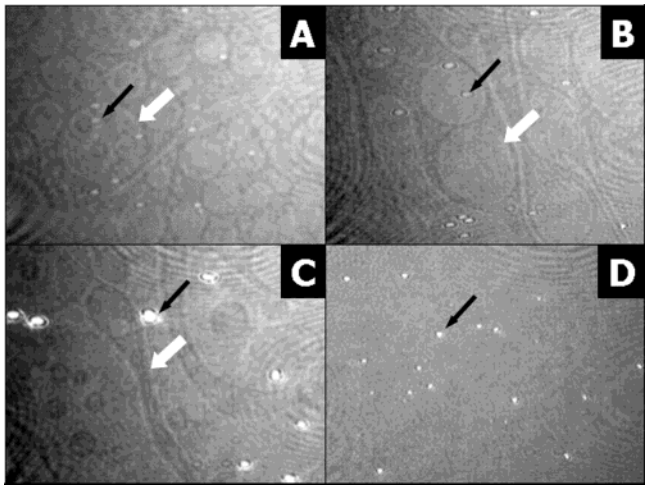

Figure 8. BAM morphologies obtained by addition and compression of a 60 wt % trisilanolisobutyl-POSS blend with PDMS (Π/mN m^{-1}, $\langle A \rangle$/Å^2 monomer^{-1}): A (10.9, 21), B (15.2, 18), and C (14, 16.5) all by addition vs D (16.5, 16.5) by compression. Solidlike domains appear bright in the images, while coexistent liquidlike phases, BAM images A → C, have much lower contrast. To highlight these features, white arrows have been added to highlight examples of thicker PDMS domains (medium brightness) on the monolayer background (darkest features), and dark arrows are used to highlight POSS aggregates (brightest, small circular domains) which tend to initially form in the thicker PDMS domains. All images are 2.4 × 3.2 mm^2 in size.

values for all of the addition data were allowed to relax until a stable, "equilibrium" surface pressure value was obtained. The "equilibrium" condition was arbitrarily chosen to be $\Delta\Pi < 0.1$ mN m^{-1} in a 10 min period. As seen in Figure 7, allowing equilibration causes the pressure to stabilize at lower values than under compression conditions. Both isotherms exhibit the same shape and trend, but the plateau pressure of the addition isotherm is lower by about 3 mN m^{-1}. Figure 8 shows the surface morphologies of the blend film at different surface pressures by addition. The surface blend film was clear before the PDMS transition and then slightly brighter round liquid domains appeared at surface pressures above about 11 mN m^{-1} (Figure 8A)—which is consistent with multilayer formation. Further addition of the mixture onto the surface leads to POSS multilayer domain formation within the upper layer of elongated PDMS bilayer domains (Figure 8B,C). Trisilanol-POSS molecules are believed to form dimers after the cusp,[35,46] as this would be a more energetically favorable conformation for POSS molecules in the hydrophobic multilayer regime. This hypothesis is supported by the known crystal structure for trisilanolcyclohexyl-POSS, where the unit cell consists of a hydrogen-bonded dimer.[40] If dimer does form at the interface, the dimeric-POSS would be nonamphiphilic, as intermolecular hydrogen bonding would replace direct hydrogen bonding between the silanol groups and water. The morphology from the compression method is shown in Figure 8D for comparison at the same surface concentration, $\langle A \rangle \sim 16.5$ Å^2 monomer^{-1}, as Figure 8C. The liquidlike multilayer domains of PDMS that appeared in addition are not observed during compression, and the condensed POSS multilayer aggregates appear to be smaller in size due to the dynamic nature of the compression process. It is important to note that the absence of liquidlike PDMS multilayer domains in Figure 8D obtained by compression does not necessarily

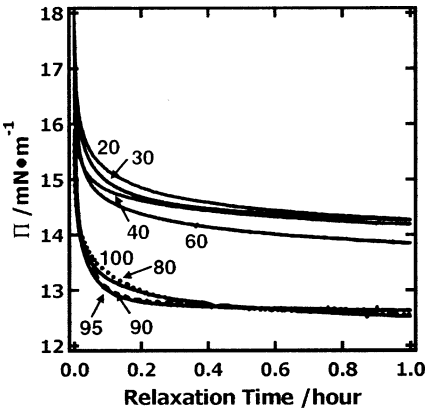

Figure 9. Relaxation, Π vs *t*, curves for blends of trisilanolisobutyl-POSS with PDMS. Compression ceased at the Π_0 values given in Table 1 for each composition ratio.

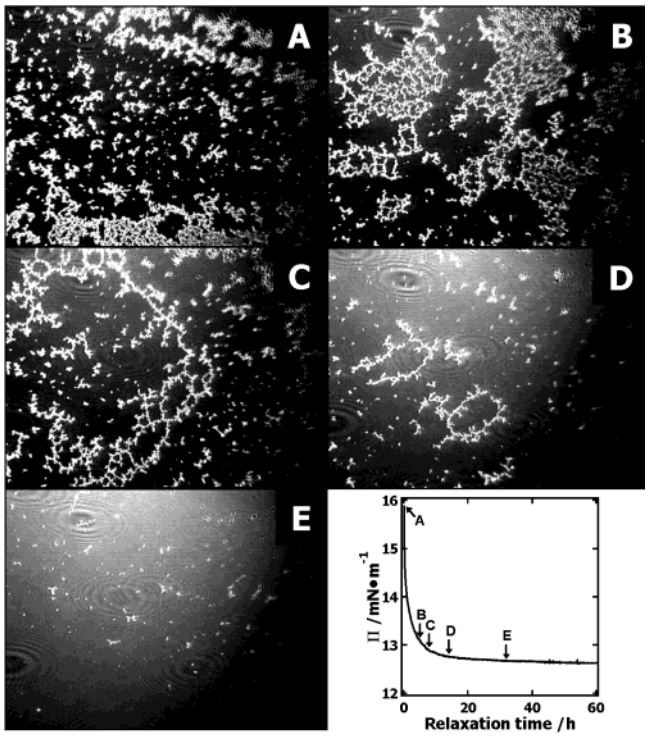

Figure 10. Morphologies obtained from a relaxation experiment for a 90 wt % POSS blend with PDMS at a constant area, $\langle A \rangle = 28.5$ Å^2 monomer^{-1}. The BAM images (A → E) correspond to the labeled points on the Π vs *t* relaxation curve. Solidlike domains appear bright in the images, which are 4.8 × 6.4 mm^2 in size.

mean that they do not exist as they could be smaller in size than the resolution of the BAM. Moreover, their presence in the addition experiments in Figure 8A−C is consistent with the long equilibration times (at least 30 min vs less than 2 min during continuous compression for comparable Π values) and lower viscosity of the film during evaporation of the spreading solvent that facilitate the formation of large domains.

Relaxation Phenomena. Figures 9−11 show representative relaxation behavior of POSS/PDMS blends. In Figure 9, the surface pressure is plotted as a function of time for representative relaxation curves. Figure 9 clearly shows two groups of data. The first group (<80 wt % POSS) corresponds to those systems that form one phase systems in the monolayer state according to the thermodynamic analysis of the isotherm data. The second group consists of those systems (>80 wt % POSS)

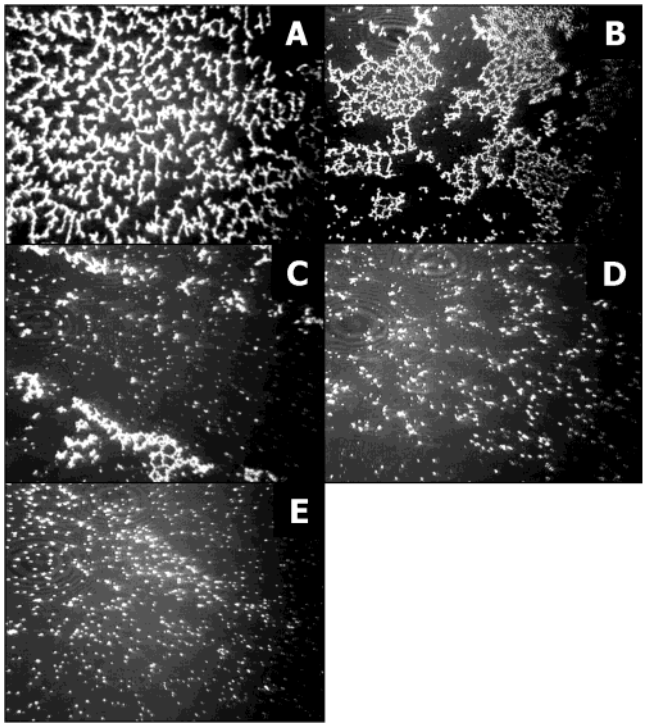

Figure 11. Blend film morphologies after 5 min of relaxation for (wt % POSS, $\langle A \rangle$/Å^2 monomer^{-1}): A (100, 60), B (90,28.5), C (80, 17.6), D (60, 11.4), and E (40, 6.7). The $\langle A \rangle$ values all correspond to a POSS concentration of $A_{POSS} \approx 60$ Å^2 molecule^{-1}. Solidlike domains appear bright in the images, which are 4.8 × 6.4 mm^2 in size.

which may form phase-separated monolayers just prior to monolayer collapse and pure trisilanolisobutyl-POSS. The high-POSS content data in Figure 9 all relax to the same final surface pressure (Π ≈ 12.5 mN m^{-1}). As this surface pressure value is comparable to pure trisilanolisobutyl-POSS, one can expect a surface where all of the PDMS is excluded from the water interface and resides on top of the POSS. In contrast, the low-POSS content films relax to a surface pressure value that is actually greater than the value obtained for pure trisilanolisobutyl-POSS. These systems suggest that both the upper and lower levels of the multilayer film contain some PDMS that enhances POSS−water interactions, thereby supporting a film with a higher surface pressure. While the molecular basis for this behavior is speculative, it is supported by BAM. Figure 10 shows representative morphological data for the relaxation of a 90:10 POSS:PDMS blend by weight following the cessation of compression. The initial pressure at the cessation of compression, Π_0, of each blend film is stated in Table 1, where both the collapse surface pressures from addition and compression are also included. As seen in Figure 9 and Table 2 for trisilanolisobutyl-POSS, there is a rapid initial relaxation in Π upon the cessation of compression and then a slower decrease in surface pressure until a stable value of Π = 12.5 mN m^{-1} is obtained. During the early stages of Π relaxation, the solidlike POSS domains aggregate into ringlike structures to minimize the contributions of line tension and dipole density to the total energy of the nonequilibrium system.[47] Representative BAM micrographs in Figure 10 for the relaxation process of a 90 wt % POSS blend show that the relaxation in Π is accompanied by the aggregation of more condensed domains to from ringlike structures at intermediate Π, before breaking up into

Table 1. Important Π Values for Trisilanolisobutyl-POSS/PDMS Blends at A/W[a]

wt % POSS	mol % POSS[b]	collapse pressure (mN m^{-1})[c]	collapse pressure (mN m^{-1})[d]	initial relaxation pressure (mN m^{-1})[e]	final relaxation pressure (mN m^{-1})[f]
0	0	8.5	8.5	8.5	8.5
20	2	18.0	13.7	17.7	14.1
30	4	17.9		17.8	14.1
40	6	17.5	13.8	16.8	14.0
60	12	17.3	13.8	15.9	12.9
80	27	17.5	12.6	15.6	12.4
90	46	17.5	12.8	15.6	12.6
95	64	17.4		16.2	12.4
100	100	17.6	12.5	15.7	12.3

[a] Π values are accurate within ±0.2. [b] mol % derived on a monomer basis, where POSS is treated as a single monomer. [c] For compression at 20 cm^2 min^{-1}. [d] For addition. [e] Initial Π_0 values for Figure 9. [f] Final Π values for Figure 9.

smaller aggregates at the lower equilibrium Π. In this respect, the behavior is the same as pure trisilanolisobutyl-POSS.[35] The ringlike structures that form during the Π relaxation process are consistent with the nonequilibrium formation of solidlike domains in a liquidlike monolayer matrix.[47]

Figure 11 shows BAM micrographs for the early stages of Π relaxation for blends of variable POSS content. Interestingly, the images in Figure 11 are nearly identical to the result seen for hysteresis experiments in Figure 6. With decreasing POSS content within the films, solidlike domains formed at A/W fail to aggregate into connected ring structures and instead form islands. This observation is further evidence for PDMS multilayer formation on top of the POSS/PDMS blend at A/W, where the water surface is not completely covered by POSS molecules upon compression. Under these conditions, PDMS molecules still could interact with POSS molecules laterally and enhance film stability as evidenced by the higher final Π values.

Returning to Figure 9, the Π−t decay curves are not single exponentials, suggesting that a complex collapse mechanism exists. The decay process is dominated by a fast relaxation process that rapidly decreases the pressure to a value near the plateau ("equilibrium") value. This fast process was assigned to a reorganization of the blend film (following its nonequilibrium compression) because the magnitude (ΔΠ) increases with both the compression rate and the target surface pressure (result not shown). This reorganization may be due to an adjustment in the distribution of dipole moments and mean distances. A process that slowly decreases Π to the plateau pressure is observed at longer times. This process was interpreted as a loss of material from the interface (or multilayer formation) and could result from a nucleation and growth process resulting in three-dimensional (3-D) aggregates.

Qualitatively, the relaxation behavior seen in Figure 9 must consist of at least a fast and a slow mode. Quantitatively, a triple-exponential function

$$\Pi/\Pi_0 = a_1 \exp(-t/\tau_1) + a_2 \exp(-t/\tau_2) + (1 - a_1 - a_2) \exp(-t/\tau_3) \quad (5)$$

where a_1 and a_2 are exponential prefactors and τ_1, τ_2, and τ_3 provide different relaxation times, was found to adequately describe the data in Figure 9. Results for the fitting parameters for different trisilanolisobutyl-POSS/PDMS blends are summarized in Table 2. The first term in eq 5, $a_1 \exp(-t/\tau_1)$, describes the initial drop in Π upon the cessation of compression. The first reorganization time, τ_1, is on the order of less than 1 min and is similar for all blend compositions (Table 2). This behavior reflects a stronger influence by the elastic rather than viscous properties of the monolayer. Hence, the first term has been attributed to local, short-range, reorganization of the functional groups of the molecules within the monolayer.

The second term in eq 5, $a_2 \exp(-t/\tau_2)$, yields a relaxation time on the order of a few minutes. In this step, there is a continuation of dipolar and chain segment relaxation along with long-range adjustment of symmetry, mean distances between domains, and the dissipation of surface pressure gradients to produce the network structures seen in Figures 10 and 11 as well as their ultimate breakup. As the prefactor, a_2, is much smaller than a_1, these processes are less significant for this system than the molecular scale rearrangements.

The final term in eq 5, $(1 - a_1 - a_2) \exp(-t/\tau_3)$, has relaxation times on the order of $\tau_3 \sim 100$ h. This term accounts for multilayer aggregation but is much longer than the experimental observation window. Hence, the prefactor defines the final plateau Π value as the experimental time scale $\ll \tau_3$. In terms of Π/Π_0 (Table 1), the percentage change in Π during relaxation increases with increasing POSS content in the film. This observation suggests that lower film viscosities accompanying the addition of PDMS minimize the importance of relaxation processes during film compression. This result is also consistent with the observed hysteresis behavior in Figure 5A.

Conclusions

One of the key remaining challenges for POSS nanotechnology is the successful blending of POSS based materials with polymers for transparent hybrid organic−inorganic nanocomposites. In this report, uniform blend monolayers of trisilanolisobutyl-POSS and PDMS could be formed up to 80 wt % POSS in the presence of an attractive surface (water). With increasing surface concentration, there is an initial departure from the monolayer state through PDMS desorption into a mul-

Table 2. Parameters Used To Fit the Relaxation of Trisilanolisobutyl-POSS/PDMS Blends

wt % POSS	a_1[a]	a_2[a]	τ_1/s[a]	τ_2/min[a]	τ_3/h[a]
20	0.1473 ± 0.0005	0.0445 ± 0.0005	30.6 ± 0.4	9.8 ± 0.2	128 ± 2
30	0.1194 ± 0.0003	0.0707 ± 0.0003	28.8 ± 0.2	7.0 ± 0.1	68 ± 1
40	0.0966 ± 0.0003	0.0481± 0.0003	28.2 ± 0.4	12.7 ± 0.2	79 ± 1
60	0.0975 ± 0.0004	0.0666 ± 0.0004	19.8 ± 0.3	9.4 ± 0.2	57 ± 1
80	0.0947 ± 0.0003	0.0934 ± 0.0003	18.6 ± 0.2	7.7 ± 0.1	96 ± 1
90	0.1015 ± 0.0002	0.0969 ± 0.0002	14.4± 0.1	3.5 ± 0.1	136 ± 1
95	0.0983 ± 0.0004	0.1098 ± 0.0004	10.2± 0.1	3.0 ± 0.1	54 ± 1
100	0.1691 ± 0.0007	0.0758 ± 0.0007	14.4± 0.2	6.8 ± 0.1	112 ± 3

[a] ±1 standard deviation.

tilayer structure. Further compression leads to desorption of trisilanolisobutyl-POSS and the formation of more condensed solidlike POSS aggregates in a PDMS fluid where one can reasonably expect POSS molecules to hydrogen bond with one another and form dimer structures as they do in bulk crystal structures.[40] Hence, this study provides insight into aggregation mechanisms that may also be important in POSS/polymer blends and coatings.

Acknowledgment. The authors appreciate the financial support of the Thomas F. Jeffress and Kate Jeffress Memorial Trust (J-553), Carilion Biomedical Institute, Virginia Tech Aspires Program, a 3M Untenured Faculty Award, the Virginia Space Grant Consortium (VSGC), the National Science Foundation (DMR-9B20274 and CHE-0239633), and the Post-doctoral Fellowship Program of the Korea Science & Engineering Foundation. The authors also thank Dr. Shawn Phillips (AFRL) for material support.

References and Notes

(1) Baney, R. H.; Sakakibara, A.; Itoh, M.; Suzuki, T. *Chem. Rev.* **1995**, *95*, 1409.
(2) Lichtenhan, J. D. *Comments Inorg. Chem.* **1995**, *17*, 115.
(3) Fu, B. X.; Hsiao, B. S.; White, H.; Rafailovich, M.; Mather, P. T.; Jeon, H. G.; Phillips, S. H.; Lichtenhan, J. D.; Schwab, J. J. *Polym. Int.* **2000**, *48*, 437.
(4) Schwab, J. J.; Lichtenhan, J. D.; Carr, M. J.; Chaffee, K. P.; Mather, P. T.; Romo-Uribe, A. *Polym. Prepr.* **1997**, *77*, 549.
(5) Gonzalez, R. I.; Philips, S. H.; Hoflund, G. B. *J. Spacecraft Rockets* **2000**, *37*, 463.
(6) Hoflund, G. B.; Gonzalez, R. I.; Philips, S. H. *J. Adhes. Sci. Tehcnol.* **2001**, *15*, 1199.
(7) Laine, R. M.; Zhang, C.; Sellinger, A.; Viculis, L. *Appl. Organomet. Chem.* **1998,** *12*, 715.
(8) Zhang, C.; Babonneau, F.; Bonhomme, C.; Laine, R. M.; Soles, C. L.; Hristov, H. A.; Yee, A. F. *J. Am. Chem. Soc.* **1998**, *120*, 8380.
(9) Fu, B. X.; Zhang, W.; Hsiao, B. S.; Rafailovich, M.; Sokolov, J.; Johansson, G.; Sauer, B. B.; Phillips, S. H.; Balnski, R. *High Perform. Polym.* **2000**, *12*, 565.
(10) Wright, M. E.; Schorzman, D. A.; Feher, F. J.; Jin, R. Z. *Chem. Mater.* **2003**, *15*, 264.
(11) Choi, J.; Kim, S. G.; Laine, R. M. *Macromolecules* **2004**, *37*, 99.
(12) Choi, J. W.; Tamaki, R.; Kim, S. G.; Laine, R. M. *Chem. Mater.* **2003**, *15*, 3365.
(13) Voronkov, M. G.; Lavrent, V. I. *Top. Curr. Chem.* **1982**, *102*, 199.
(14) Lichtenhan, J. D.; Vu, N. Q.; Carter, J. A.; Gilman, J. W.; Feher, F. J. *Macromolecules* **1993**, *26*, 2141.
(15) Haddad, T. S.; Lichtenhan, J. D. *J. Inorg. Organomet. Polym.* **1995**, *5*, 237.
(16) Gilman, J. W.; Schlitzer, D. S.; Lichtenhan, J. D. *J. Appl. Polym. Sci.* **1996**, *60*, 591.
(17) Haddad, T. S.; Viers, B. D.; Phillips, S. H. *J. Inorg. Organomet. Polym.* **2001**, *11*, 155.
(18) Scott, D. W. *J. Am. Chem. Soc.* **1946**, *68*, 356.
(19) Hacker, N. P. *MRS Bull.* **1997**, *22*, 33.
(20) Leu, C. M.; Chang, Y. T.; Wei, K. H. *Macromolecules* **2003**, *36*, 9122.
(21) Leu, C. M.; Chang, Y. T.; Wei, K. H. *Chem. Mater.* **2003**, *15*, 3721.
(22) Haddad, T. S.; Lichtenhan, J. D. *Macromolecules* **1996**, *29*, 7302.
(23) Xu, H. Y.; Kuo, S. W.; Lee, J. S.; Chang, F. C. *Macromolecules* **2002**, *35*, 8788.
(24) Mantz, R. A.; Jones, P. F.; Chaffee, K. P.; Lichtenhan, J. D.; Gilman, J. W.; Ismail, I. M. K.; Burmeister, M. J. *Chem. Mater.* **1996**, *8*, 1250.
(25) Kim, G. M.; Qin, H.; Fang, X.; Sun, F. C.; Mather, P. T. *J. Polym. Sci., Part B: Polym. Phys.* **2003**, *41*, 3299.
(26) Li, G. Z.; Wang, L. C.; Ni, H. L.; Pittman, C. U. *J. Inorg. Organomet. Polym.* **2001**, *11*, 123.
(27) Sarantopoulou, E.; Kollia, Z.; Kocevar, K.; Musevic, I.; Kobe, S.; Drazic, G.; Gogolides, E.; Argitis, P.; Cefalas, A. C. *Mater. Sci. Eng. C* **2003**, *23*, 995.
(28) Jakubek, V.; Liu, X. Q.; Vohra, V. R.; Douki, K.; Kwark, Y. J.; Ober, C. K.; Markley, T. J.; Robertson, E. A.; Carr, R. V. C.; Marsella, J. A.; Conley, W.; Miller, D.; Zimmerman, P. *J. Photopolym. Sci. Technol.* **2003**, *16*, 573.
(29) Waddon, A. J.; Coughlin, E. B. *Chem. Mater.* **2003**, *15*, 4555.
(30) Waddon, A. J.; Zheng, L.; Farris, R. J.; Coughlin, E. B. *Nano Lett.* **2002**, *2*, 1149.
(31) Ogarev, V. *Colloid, J.* **2001**, *63*, 445.
(32) Kobayashi, H. *Makromol. Chem.* **1993**, *194*, 2569.
(33) Knischka, R.; Dietsche, F.; Hanselmann, R.; Frey, H.; Mulhaupt, R. *Langmuir* **1999**, *15*, 4752.
(34) Deng, J.; Polidan, J. T.; Hottle, J. R.; Farmer-Creely, C. E.; Viers, B. D.; Esker, A. R. *J. Am. Chem. Soc.* **2002**, *124*, 15194.
(35) Deng, J.; Hottle, J. R.; Polidan, J. T.; Kim, H. J.; Farmer-Creely, C. E.; Viers, B. D.; Esker, A. R. *Langmuir* **2004**, *20*, 109.
(36) Fox, H. W.; Taylor, W.; Zisman, W. A. *Ind. Eng. Chem.* **1947**, 1401.
(37) Mann, E. K.; Langevin, D. *Langmuir* **1991**, *7*, 1112.
(38) Lee, L. T.; Mann, E. K.; Langevin, D.; Farnoux, B. *Langmuir* **1991**, *7*, 3076.
(39) Mann, E. K.; Hénon, S.; Langevin, D.; Meunier, J. *J. Phys., II* **1992**, *2*, 1683.
(40) Feher, F. J.; Newman, D. A.; Walzer, J. F. *J. Am. Chem. Soc.* **1989**, *111*, 1741.
(41) Gaines, G. L. *Insoluble Monolayers at Liquid−Gas Interfaces*; Wiley: New York, 1966.
(42) Goodrich, F. C. *Proc. 2nd Int. Congr. Surf. Activity* **1957**, 85.
(43) Flory, P. J. *J. Chem. Phys.* **1942**, *10*, 51.
(44) Atkins, P. *Physical Chemistry*, 6th ed.; Freeman: New York, 1998.
(45) Miller, A.; Möhwald, H. *J. Chem. Phys.* **1987**, *86*, 4258.
(46) Deng, J.; Farmer-Creely, C. E.; Viers, B. D.; Esker, A. R. *Langmuir* **2004**, *20*, 2527.
(47) McConnell, H. M.; Tamm, L. K.; Weiss, R. M. *Proc. Natl. Acad. Sci. U.S.A* **1984**, *81*, 3249.

MA049511M